ELSEVIER

Contents lists available at ScienceDirect

# Journal of Chromatography Open

journal homepage: www.elsevier.com/locate/jcoa



# Orthogonality of separation and sorbent evaluation in offline multidimensional peptide fractionation using automated positive pressure micro solid phase extraction

Renata Biba <sup>a,1</sup>, Karla Košpić <sup>b,1,2</sup>, Blaž Ivšić <sup>a</sup>, Lucija Vujević <sup>a</sup>, Amela Hozić <sup>a</sup>, Marijana Erk <sup>a</sup>, Irena Đapić <sup>a</sup>, Mario Cindrić <sup>a,\*</sup>

#### ARTICLE INFO

# Keywords: Peptide fractionation Sorbent Multidimensional micro solid phase extraction Orthogonality Mutual information Informational entropy

#### ABSTRACT

Micro solid-phase extraction (µSPE) is a simple and efficient method for peptide separation, purification, and fractionation prior to mass spectrometry (MS) in bottom-up proteomics workflows. Here, we introduce a positive-pressure (PP)-µSPE platform for offline multidimensional peptide fractionation. Six one-dimensional (1D) fractionation protocols were optimized at low pH reversed-phase (RP), high pH RP, strong cation exchange (SCX), hydrophilic-lipophilic balance (HLB), quaternary methyl-ammonium (QMA), and mixed strong anion exchange/reversed-phase (MAX) using bovine serum albumin (BSA) tryptic peptides. Each protocol yielded six fractions, which were evaluated by peptide size, isoelectric point, and hydrophilicity. Peptide fractions were separated on nano-C18 RP column and analyzed by nanoESI-QTOF-MS, and fractionation performance was subsequently evaluated for each fractionation mode. The data were then paired to quantify orthogonality in projected multidimensional fractionation by employing information theory. QMA yielded the highest entropy, indicating the greatest peptide dispersion in 1D. Conversely, high pH RP fractionation had the lowest entropy and led to increased peptide modification and aggregation, compromising downstream analysis. Joint entropy and mutual information analysis identified the most orthogonal pairings (QMA-low pH RP, MAX-QMA, HLB-QMA) and highlighted redundancy among methods sharing similar separation mechanisms. Workflow's practical utility was demonstrated on the fragment antigen-binding part of Cetuximab, where QMA fractionation enabled identification of a previously undetected heavy chain peptide, achieving complete sequence coverage. These results demonstrate that PP-µSPE enables repeatable and combinable peptide fractionation across diverse sorbents and complex proteins, and supports targeted workflows by facilitating selective peptide isolation based on their physicochemical properties, streamlining experimental design in multidimensional proteomic analyses.

# 1. Introduction

Recent technological advances in mass spectrometry (MS) instrumentation have enabled rapid, in-depth analysis of proteins across a wide range of biological samples [1–3]. However, the high complexity and a broad range of protein abundance still exceed the separation capacity of most analytical systems, which limits protein identification [4]. Therefore, to simplify the peptide mixture and enable detection of low abundant species, peptide fractionation is frequently used prior to

MS analysis in the bottom-up proteomic workflows. Moreover, peptide fractionation improves proteome coverage and enhances resolving power, contributing to more accurate protein identification [5,6]. Although gel electrophoresis-based methods, such as sodium dodecyl sulfate-polyacrylamide gel electrophoresis (SDS-PAGE) and isoelectric focusing (IEF), can be used to resolve complex protein mixtures, chromatography-based systems now prevail due to their flexible configuration, higher sample loading capacity, and the possibilities for automation and MS hyphenation [7,8].

a Ruđer Bošković Institute, Bijenička cesta 54, 10000, Zagreb, Croatia

<sup>&</sup>lt;sup>b</sup> Faculty of Biotechnology and drug development, University of Rijeka, Radmile Matejčić 2, 51000, Rijeka, Croatia

<sup>\*</sup> Corresponding author at: Division of Molecular Medicine, Ruđer Bošković Institute, 10 000, Zagreb, Croatia *E-mail address:* mario.cindric@irb.hr (M. Cindrić).

 $<sup>^{1}\,</sup>$  These authors have equally contributed to this manuscript.

<sup>&</sup>lt;sup>2</sup> Present address: BICRO BIOCentre Ltd, Central Lab, Borongajska cesta 83 H, 10000 Zagreb, Croatia

Multidimensional liquid chromatography (2D or 3D-LC), implemented in online, offline, or partially coupled formats, is often employed to overcome the sample loading and sensitivity limitations of micro- and nanoLC-MS platforms which can hinder the detection of low-abundance proteins. Its main advantage lies in the flexibility to optimize separation conditions in each dimension, including stationary and mobile phase composition, to match the properties of the analyzed sample [9,10]. Two configurations aim to couple orthogonal separation mechanisms to enhance the separation power, most commonly strong cation exchange (SCX) [11,12], high pH reverse phase (RP) chromatography [13], size-exclusion chromatography (SEC) [14,15] or hydrophilic interaction chromatography (HILIC) [16,17] in the first dimension with low pH RP-LC in the second. In online setups, solvent compatibility can be a challenge when hyphenating LC columns in 2D systems or with downstream MS coupling, often limiting the range of viable column combinations [9,18]. In contrast, offline 2D-LC offers greater control over separation conditions in each dimension, resulting in improved peptide distribution [9,19]. Additionally, it allows for selective fraction collection and concatenation, enhancing sensitivity in downstream applications such as post-translational modification analysis, targeted proteomics, and biomarker discovery [20-22].

However, introducing multidimensionality in peptide fractionation protocols, particularly in offline formats, can introduce errors in quantitative analysis. Each additional dimension increases the risk of sample loss and artefacts, such as peptide degradation, potentially resulting in lower sequence coverage and significant reproducibility issues [23]. Automated solid phase extraction (SPE) enhances both the speed and reproducibility of sample processing, making it highly applicable in proteomics workflows. Namely, SPE has proven to be highly selective and efficient in peptide isolation, purification, enrichment and fractionation protocols [24–30], but is still not routinely implemented in multidimensional fractionation. The current availability of diverse SPE sorbents, combined with the full independence of each dimension, can significantly enhance multidimensional workflows by empowering the combinations of truly orthogonal separation mechanisms.

Theoretically, the separation performance in an orthogonal multidimensional approach should be the product of the individual separation principle applied. However, there are certain practical limitations that hinder the achievable peak capacity, mainly due to secondary interactions between the sorbent and analyte. This can prevent proper elution and increase overlap between different separation methods resulting in reduced separation orthogonality [9,31]. Therefore, quantification of separation orthogonality represents a critical aspect in the development and evaluation of multidimensional LC workflows. However, although frequently referenced in papers when comparing separation performance in multidimensional approaches, orthogonality still lacks the formal definition in chromatography as well as standardized metrics for comparing datasets across multiple dimensions [32]. Different approaches have been proposed to capture either the extent of occupied separation space or the uniformity of peak distribution [33]. For example, Gilar et al. [31] introduced a straightforward geometric approach, proposing an orthogonality measure based on the total number of bins in the 2D chromatography space and the number of bins occupied by peptide peaks. Alternative methods utilize information theory to measure orthogonality [34,35], offering the advantage of accounting for off-diagonal correlations. For evaluation of orthogonality in multidimensional SPE fractionation approach proposed in this paper, we adopt combination of entropy and mutual information to measure orthogonality, as it provides both simplicity and the aforementioned advantages.

Here, we present a novel approach to offline multidimensional peptide fractionation using an automated positive pressure micro solid phase extraction (PP-µSPE) platform that enables sample preparation with minimal user intervention and offers low solvent consumption, reduced intrinsic costs and decreased processing time. Bovine serum albumin (BSA) tryptic peptides were selected as a model system because

of a broad spectrum of their physicochemical properties which allow for systematic evaluation of different  $\mu SPE$  fractionation methods. Specifically, the digest yields approximately 100 peptides that differ in length (6 – 31 amino acids), isoelectric point (pI, 3.8 – 10) and grand average of hydropathy (GRAVY) index (-2 – 1.4). The objective of this study was to employ the named platform to systematically evaluate separation orthogonality of BSA tryptic peptides within multidimensional peptide fractionation dataspace through three main steps:

- Evaluation of fractionation performance of six distinct μSPE fractionation methods high pH RP, low pH RP, SCX, hydrophilic-lipophilic balance (HLB), quaternary methyl-ammonium (QMA), and mixed strong anion exchange/reversed-phase (MAX) based on peptide physicochemical properties: pI, GRAVY index, and peptide length.
- Data pairing and development of orthogonality metrics between tested fractionation pairs in 2D-uSPE.
- Identification of the most effective fractionation combinations for multidimensional workflows.

Finally, to demonstrate applicability of the optimized fractionation workflow for complex samples, we applied it to the fragment antigenbinding (Fab) portion of the pharmaceutically relevant monoclonal antibody (mAb) Cetuximab, with the aim of improving sequence coverage.

# 2. Materials and methods

#### 2.1. Chemicals and materials

Ammonium bicarbonate, BSA, formic acid (FA), leucine enkephalin (LE), isopropanol, trypsin from porcine pancreas, ammonium hydroxide, and trifluoroacetic acid (TFA) were obtained from Sigma-Aldrich (St. Louis, MO, USA). Acetonitrile (ACN), tris(2-carboxyethyl) phosphine (TCEP), methanol, and ammonium acetate were obtained from Merck Millipore (Darmstadt, Germany). Ammonium formate was obtained from Honeywell (Charlotte, North Carolina, USA). Guanidine hydrochloride (GuaHCl) was obtained from Avantor (Radnor Township, PA, USA). Cetuximab (Erbitux®) was obtained from Merck (Rahway, NJ, USA). RapiGest SF and RapiZyme Trypsin were purchased from Waters (Milford, MA, USA), Ultrapure water (18 M $\Omega$  cm) was produced in-house using Milli-Q system Direct-Q® 3UV from Merck Millipore. Resin-free AssayMAP cartridges (5 µL; Agilent Technologies, St. Clara, CA, USA) were packed in-house with non-standardized sorbents using a dry-fill high-pressure method. Briefly, the weighed material was loaded onto each cartridge and compressed with air at 2.5 bar. Oasis HLB (60 μm, 80 Å), Oasis MAX (60 μm, 80 Å), and Sep-Pak AcellPlus QMA (37 -55 μm, 300 Å) sorbents were obtained from Waters (Milford, MA, USA), Bondesil SCX (40 µm, 300 Å) was obtained from Agilent Technologies (St. Clara, CA, USA) and Sepra  $^{TM}$  C18-E (50  $\mu m,\,65$  Å) was obtained from Phenomenex (Torrance, CA, USA).

# 2.2. Peptide preparation

BSA protein solution was prepared at 1 mg mL<sup>-1</sup> in 50 mM ammonium bicarbonate buffer (pH 7.8) and reduced with TCEP (final concentration 5 mM) for 15 min at room temperature. After reduction, trypsin (1:50 w/w) solution was added, and digestion was carried out in a thermomixer (Eppendorf, Hamburg, Germany) for 18 h at 37°C and 350 rpm. The BSA tryptic peptide solution was then aliquoted into tubes containing 10  $\mu$ g of peptides each, and dried using a vacuum centrifuge (Eppendorf, Hamburg, Germany).

Cetuximab was prepared at 1 mg mL $^{-1}$  in 6 M GuaHCl, 50 mM TrisHCl (pH 8.0) and incubated at room temperature for 10 min. RapiGest SF (final concentration 0.1 % w/v) was added and incubated for an additional 10 min, followed by reduction with TCEP (final concentration

10 mM) for 60 min. The sample was then diluted 5-fold in 50 mM ammonium bicarbonate buffer (pH 7.8) and digested for 18 hours at 37°C with RapiZyme (1:20, w/w). Digestion was quenched with 1 % FA, which also precipitated excess RapiGest. The precipitate was removed by centrifugation, and the resulting peptide mixture was desalted and concentrated on the AssayMAP Bravo Platform (Agilent Technologies, St. Clara, CA, USA) using in-house packed C18-E cartridges. For cleanup, cartridges were conditioned with 100  $\mu$ L of 50 % ACN in 0.1 % TFA at 300  $\mu$ L min $^{-1}$  flow rate, and loaded with 100  $\mu$ L of the Cetuximab digest at 10  $\mu$ L min $^{-1}$ . Bound peptides were washed with 0.1 % TFA and eluted with 25  $\mu$ L of 80 % ACN in 0.1 % TFA at a flow rate of 10  $\mu$ L min $^{-1}$ . The eluate was vacuum dried and split into two aliquots – one used directly for MS analysis and the other subjected to QMA fractionation.

#### 2.3. Peptide fractionation

Peptide fractionation was done on the AssayMAP Bravo Platform, using in-house prepared cartridges. All fractionation protocols followed a unified workflow, starting with conditioning of the sorbent using 100  $\mu L$  of the corresponding priming buffer (Table 1) at 300  $\mu L$  min $^{-1}$  flow rate, followed by 100  $\mu L$  of the equilibration buffer at 100  $\mu L$  min $^{-1}$  flow rate. Next, 100  $\mu L$  of the peptide mixture was loaded onto the sorbent at a flow rate of 10  $\mu L$  min $^{-1}$  and the non-specifically or loosely bound contaminants were washed with 100  $\mu L$  of equilibration buffer. Fractionation was done using 6 elution buffers specific to the chosen sorbent chemistry, and 25  $\mu L$  fraction was collected every 2.5 min resulting in 6 fractions. Each fraction was vacuum dried and stored at  $-80\,^{\circ}\text{C}$  prior to the MS analysis.

For method development, BSA tryptic peptides were fractionated using all six sorbent chemistries described in Table 1. Cetuximab tryptic peptides were fractionated only on QMA cartridges, following the same workflow and buffer compositions.

# 2.4. Nano-ultra-performance liquid chromatography-electrospray ionization-quadrupole mass spectrometry analysis

Dried BSA peptide fractions and Cetuximab peptides, both fractionated and cleaned up only, were reconstituted in 25  $\mu L$  of 0.1 % FA for the MS analysis. Peptides were separated on a nanoAcquity UPLC system equipped with a nanoAcquity UPLC 2D-V/M symmetry C18 trap column (100 Å, 5  $\mu m$ , 180  $\mu m \times 20$  mm) and a nanoAcquity UPLC BEH C18 analytical column (130 Å, 1.7  $\mu m$ , 100  $\mu m \times 100$  mm) with the column temperature set at 40°C. Injection volume was set to 0.6  $\mu L$  for all samples. Mobile phase A consisted of 0.1 % FA ( $\nu/\nu$ ) in MQ-H<sub>2</sub>O, and mobile phase B was 0.1 % FA ( $\nu/\nu$ ) in 95 % ( $\nu/\nu$ ) ACN. Isocratic delivery of solvent A into the trap column was performed at a flow rate of 15  $\mu L$ 

min $^{-1}$  during 2 min. The samples were eluted under gradient elution conditions at a flow rate of 1  $\mu L$  min $^{-1}$  and a total run time of 32 min. The following elution gradient was used: 0-3 min, 80 % solvent A; 3-24 min, 45 % solvent A; 24-27 min, 1 % solvent A; 27-29 min, 80 % solvent A; and 29-32 min, 80 % solvent A. The modifier solution, consisting of 1 mM ethyl methanoate in isopropanol was introduced from the Synapt channel A into the capillary sample flow via a "T" connector at a flow rate of 0.4  $\mu L$  min $^{-1}$ .

A nanoUPLC system was coupled to a nanoESI-QTOF Synapt G2-Si mass spectrometer, and the instrument parameters were set using MassLynx software (v4.1). Acquisition mode for both MS and MS<sup>E</sup> was set to positive polarity and resolution analyzer mode. The parameters were set as follows: nitrogen flow was 1.2 bar with a source temperature of 80°C, and the capillary voltage was set to 4.3 kV. Cone voltage was set to 40 kV for both MS and MS<sup>E</sup> and spectral acquisition time was 1 s. Collision energy during MS<sup>E</sup> analysis was set on 4 V for the low energy trap function and ramped from 20 to 45 V for the high energy trap function. A solution of 1 ng  $\mu L^{-1}$  leucine enkephalin in 50 % (v/v) isopropanol in MQ-H<sub>2</sub>O containing 0.1 % FA (v/v) was continuously infused from the Synapt channel B to ensure mass accuracy of the scans. NanoUPLC-nanoESI-QTOF instrument and software were produced by Waters (Milford, MA, USA).

# 2.5. Data processing

Fraction MS<sup>E</sup> spectra obtained by nanoUPLC-nanoESI-QTOF instrument were processed with MassLynx software (v4.1, Waters) and analyzed using ProteinLynx Global Server (PLGS, v.3.0.1, Waters). For BSA peptides, experimental spectra were matched to theoretical spectra derived from the Bos taurus reference proteome (Uniprot, ID UP000009136), while Cetuximab Fab spectra were matched to its heavy and light chain sequences (Protein data bank, PDB IDs: 1yypD and 1yypC) with False Discovery Rate < 1 %. The list of potential modifications for BSA included methionine oxidation, asparagine deamidation, glutamine deamidation, and serine/threonine dehydration. For Cetuximab analysis, serine/threonine/tyrosine phosphorylation, cysteine/ acid/glutamic acid/histidine/lysine/asparagine/arginine/ glutamine methylation, phenylalanine oxidation, and O-GlcNAc modifications were also added. Retention times of eluted peptides were adjusted to a continuous scale across fractions. Since each fraction LC run was 32 min, adjusted retention times were calculated as:

$$RT_{adjusted} = RT_{measured} + (n-1) \times 32$$
 (1)

where *n* is the fraction number. After obtaining the list of identified peptides in each fraction of each tested fractionation mode, sequence coverage per fraction as well as total sequence coverage were calculated for both BSA and Cetuximab Fab. Furthermore, ProtParam tool (Expasy,

Table 1
Buffer compositions for priming, equilibration, and elution steps in PP-μSPE of tryptic peptides. Conditions are specified for each fractionation method, including MAX, SCX, HLB, QMA, low pH RP, and high pH RP.

|                  | • '                 | 0 1  |              |  |                                |                                   |
|------------------|---------------------|--|--------------|--|--------------------------------|-----------------------------------|
|                  | MAX                 | SCX  | HLB          | QMA  | Low pH RP                      | High pH RP                        |
| Priming buffer   | 100 % MeOH          | 400 mM NH4HCOO with 1 %                            | 100 % MeOH   | 400 mM NH4HCOO with 1 %                            | 20 mM NH4HCOO, pH              | 20 mM NH₄HCOO, pH                 |
|                  |                     | FA in 25 % ACN                                     |              | NH <sub>4</sub> OH in 25 % ACN                     | 2.5, in 50 % ACN               | 10, in 50 % ACN                   |
| Equilibration    | MQ-H <sub>2</sub> O | 1 % FA in 25 % ACN                                 | 1 % FA       | 1 % NH <sub>4</sub> OH                             | 20 mM NH <sub>4</sub> HCOO, pH | 20 mM NH <sub>4</sub> HCOO, pH 10 |
| buffer           |                     |  |              |  | 2.5                            |                                   |
| Elution buffer 1 | 3 % ACN in 1        | 40 mM NH <sub>4</sub> HCOO, pH 3.5, in             | 5 % ACN in 1 | 20 mM NH <sub>4</sub> CH <sub>3</sub> COO in 25 %  | 20 mM NH <sub>4</sub> HCOO, pH | 20 mM NH₄HCOO, pH                 |
|                  | % TFA               | 25 % ACN   | % FA         | MeOH   | 2.5, in 15 % ACN               | 10, in 5 % ACN                    |
| Elution buffer 2 | 9 % ACN in 1        | 40 mM NH <sub>4</sub> HCOO, pH 4.0, in             | 10 % ACN in  | 40 mM NH <sub>4</sub> CH <sub>3</sub> COO in 25 %  | 20 mM NH4HCOO, pH              | 20 mM NH₄HCOO, pH                 |
|                  | % TFA               | 25 % ACN   | 1 % FA       | MeOH   | 2.5, in 20 % ACN               | 10, in 8 % ACN                    |
| Elution buffer 3 | 13 % ACN in         | 40 mM NH <sub>4</sub> CH <sub>3</sub> COO, pH 4.5, | 15 % ACN in  | 80 mM NH <sub>4</sub> CH <sub>3</sub> COO in 25 %  | 20 mM NH <sub>4</sub> HCOO, pH | 20 mM NH <sub>4</sub> HCOO, pH    |
|                  | 1 % TFA             | in 25 % ACN  | 1 % FA       | MeOH   | 2.5, in 25 % ACN               | 10, in 10 % ACN                   |
| Elution buffer 4 | 20 % ACN in         | 40 mM NH <sub>4</sub> CH <sub>3</sub> COO, pH 5.0, | 20 % ACN in  | 150 mM NH <sub>4</sub> CH <sub>3</sub> COO in 25 % | 20 mM NH <sub>4</sub> HCOO, pH | 20 mM NH <sub>4</sub> HCOO, pH    |
|                  | 2 % TFA             | in 25 % ACN  | 1 % FA       | MeOH   | 2.5, in 30 % ACN               | 10, in 15 % ACN                   |
| Elution buffer 5 | 30 % ACN in         | 40 mM NH <sub>4</sub> CH <sub>3</sub> COO, pH 6.0, | 30 % ACN in  | 200 mM NH <sub>4</sub> CH <sub>3</sub> COO in 25 % | 20 mM NH <sub>4</sub> HCOO, pH | 20 mM NH <sub>4</sub> HCOO pH 10, |
|                  | 2 % TFA             | in 25 % ACN  | 1 % FA       | MeOH   | 2.5, in 35 % ACN               | in 20 % ACN                       |
| Elution buffer 6 | 50 % ACN in         | 100 mM NH <sub>4</sub> OH, pH 9.5, in              | 40 % ACN in  | 40 mM NH <sub>4</sub> HCOO, pH 3.5, in             | 20 mM NH <sub>4</sub> HCOO, pH | 20 mM NH <sub>4</sub> HCOO, pH    |
|                  | 3 % TFA             | 25 % ACN   | 1 % FA       | 25 % MeOH  | 2.5, in 45 % ACN               | 10, in 25 % ACN                   |
|                  |                     |  |              |  |                                |                                   |

Swiss Bioinformatics Resource Portal) was used to calculate theoretical pI and GRAVY index for each identified BSA peptide.

# 2.6. BSA data preparation

All signal processing was performed in MATLAB R2011b (Statistics and Machine Learning Toolbox).

## 2.6.1. BSA peptide selection and filtering

Database search returned 64, 69, 68, 60, 69 and 72 peptides for the MAX, SCX, HLB, QMA, low pH RP and high pH RP methods, respectively (402 intensity profiles). To enable direct cross-method comparison, only peptides detected in all methods were retained, leaving 49 peptides (294 profiles).

# 2.6.2. Intensity profiles and fraction assignment

For each detected BSA peptide, TIC-normalised,  $log_2$ -transformed intensities were fitted to a normal distribution with fitdist(..., 'Normal'). The fitted mean  $(\mu)$  was rounded to the nearest whole number—ties resolved toward the fraction with the higher intensity—to assign the peptide to its most probable elution fraction.

#### 2.6.3. Construction of distribution matrices

To assess the orthogonality of any pair of fractionation methods, *i.e.*, separation mechanisms, we formed a 6  $\times$  6 matrix where each cell (i,j) represents the count of peptides assigned to fraction i in the first method and fraction j in the second method. This matrix was normalized (divided by the total peptide count) to obtain a joint probability distribution P(i,j). Additionally, marginal  $(1\times 6)$  distributions P(i) for each individual method were extracted by summing over the corresponding rows or columns of the 6  $\times$  6 matrix.

# 2.7. Entropy and mutual information

Following the definitions in [36], we treated the fraction assignments of a peptide under each method as discrete random variables taking values in  $\{1, 2, 3, 4, 5, 6\}$ . Specifically:

# 2.7.1. Joint entropy

The joint entropy  $H(M_1,M_2)$  for a pair of methods  $M_1$  and  $M_2$  was computed from the joint probability distribution:

$$H(M_1, M_2) = -\sum_{i=1}^{6} \sum_{i=1}^{6} P(i, j) \log_2(P(i, j))$$
 (2)

Here, P(i,j) denotes the probability that a peptide is assigned to fraction i in method  $M_1$  and fraction j in method  $M_2$ .

# 2.7.2. Marginal entropies

From the same data, the marginal entropies  $H(M_x)$  were obtained in a similar way:

$$H(M_x) = -\sum_{i=1}^{6} P(i)\log_2(P(i))$$
 (3)

Where P(i) denotes the probability that a peptide is assigned to fraction i in method  $M_x$ .

# 2.7.3. Mutual information

The mutual information  $I(M_1,M_2)$  between the two methods was then obtained by:

$$I(M_1; M_2) = H(M_1) + H(M_2) - H(M_1, M_2)$$

$$= \sum_{i=1}^{6} \sum_{j=1}^{6} P(i, j) \log_2 \left( \frac{P(i, j)}{P(i) P(j)} \right)$$
(4)

## 3. Results and discussion

# 3.1. Peptide fractionation optimization

Introducing multidimensionality into chromatographic separation significantly enhances the resolving power for complex peptide mixtures, such as those derived from tryptic digestion [37-39]. However, optimizing peptide distribution within a single separation dimension remains a key requirement for achieving high orthogonality values in multidimensional approach. As previously reported [10], application of nonlinear gradients remains the most common approach in peptide distribution equalization. Therefore, in our study, the first step was to optimize the 1D-µSPE protocols for the fractionation of BSA tryptic peptides using different sorbent chemistries (MAX, SCX, HLB, QMA, low pH RP and high pH RP) by adjusting the buffer compositions for elution steps (Table 1) to obtain 6 fractions for each individual method. The strong linear correlation of retention times between replicate injections (shown for HLB in Fig. S1) demonstrates the high repeatability and retention time stability of the PP-uSPE-based peptide fractionation workflow. Obtained base peak intensity (BPI) chromatograms (Fig. 1, Fig. S2 – S6) and BSA peptide intensity distribution graphs (Fig. 2) after subsequent RPLC-MS analysis of each fraction show that six fractions were obtained in each 1D-µSPE. In general, higher peptide counts were recorded in the middle fractions compared to the first and last one, which was further corroborated by a lower percentage of sequence coverage of BSA protein obtained from fractions 1 and 6 compared to that of fractions 2, 3, 4 and 5 (Table S1). To address the fact that some peptides were detected across multiple fractions, we fitted normal distribution to the intensity profile and determined the mean fraction as explained in the section 2.6.2. As a result, MAX, HLB, and high pH RP fractionation modes yielded five fractions containing unique peptides, which was accounted for in the downstream analyses. Peptide detection across multiple fractions is common in multidimensional fractionation workflows [40-42]. While it can complicate interpretation, it also enhances proteome coverage and detection of low-abundance peptides. Modern bioinformatic pipelines account for such redundancy, and in pharmaceutical applications, such as monoclonal antibody characterization, overlap can improve sequence coverage and confidence in structural assignments.

# 3.2. Influence of peptide physicochemical parameters on fractionation profiles in $\mu SPE$

The concept of sample dimensionality is highly evident for the mixture of tryptic peptides in terms of their heterogeneous physicochemical properties, which can be seen from the BSA peptide fraction distribution graphs based on peptide length (Fig. 3), GRAVY index (Fig. 4) and pI (Fig. 5). Among these, peptide length proves to be the dominant dimension affecting peptide retention, as evidenced by a distinct positive correlation between fraction number and peptide length observed in all tested fractionation methods, with the exception of high pH RP (Fig. 3). Hydrophobicity and net charge play significant roles in peptide distribution in RPLC and IEX fractionation methods, respectively. However, there are considerable deviations attributed to the peptide size effects as longer peptide chains (< 15 amino acids) contain more diverse residues which can interact differently with the sorbent during the fractionation [43]. These size-related effects are more pronounced in pI-based peptide distributions since GRAVY index inherently accounts for peptide length.

In the HLB, low pH RP and high pH RP fractionation methods a clear trend of increasing peptide hydrophobicity is observed in the later fractions, reflecting the stronger interaction of hydrophobic peptides with the sorbent and their subsequent elution with higher concentrations of the organic eluent (Fig. 4A, 4B and 4C) [44,45]. Notably, HLB fractionation appeared to be largely independent of peptide pI, likely due to the ion-pairing effects of FA present in the elution buffers

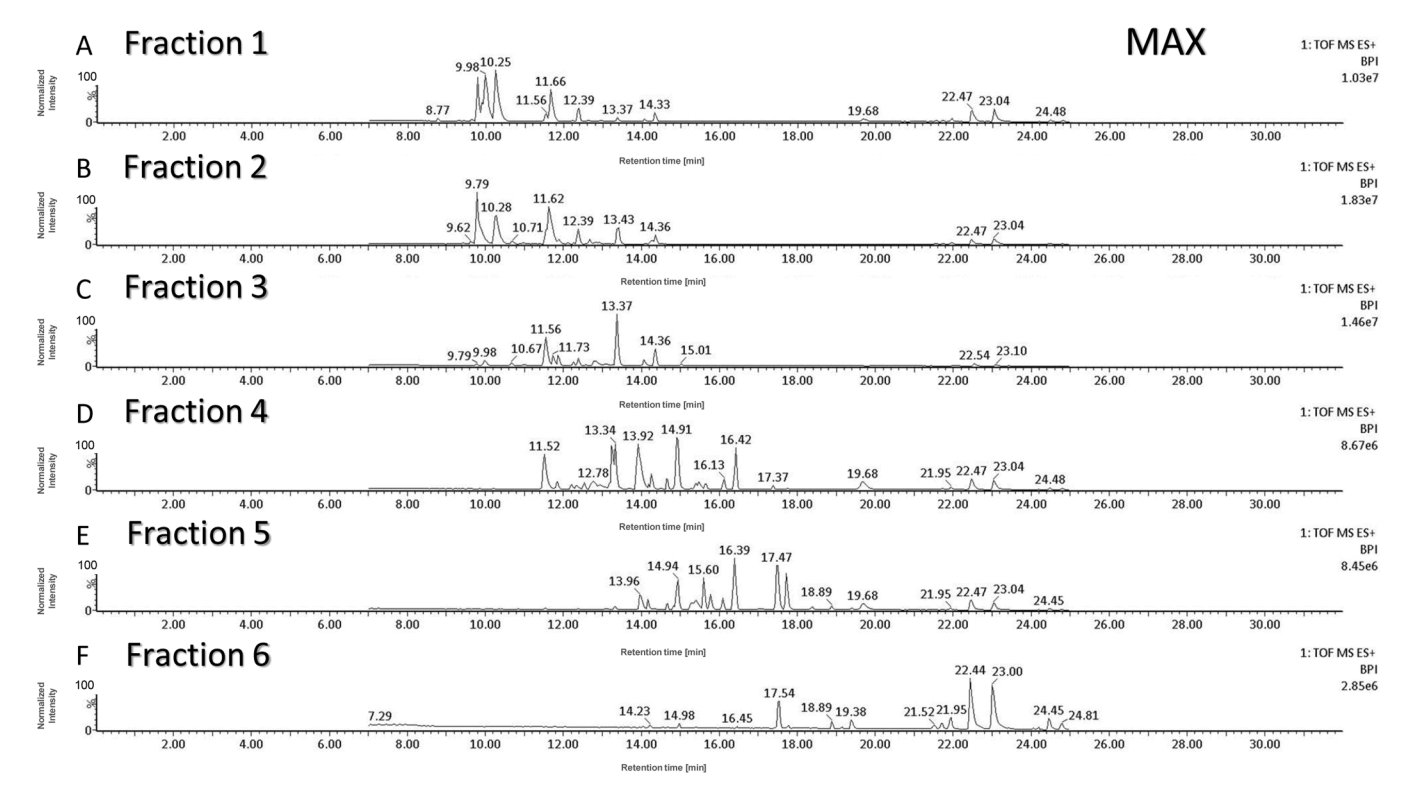
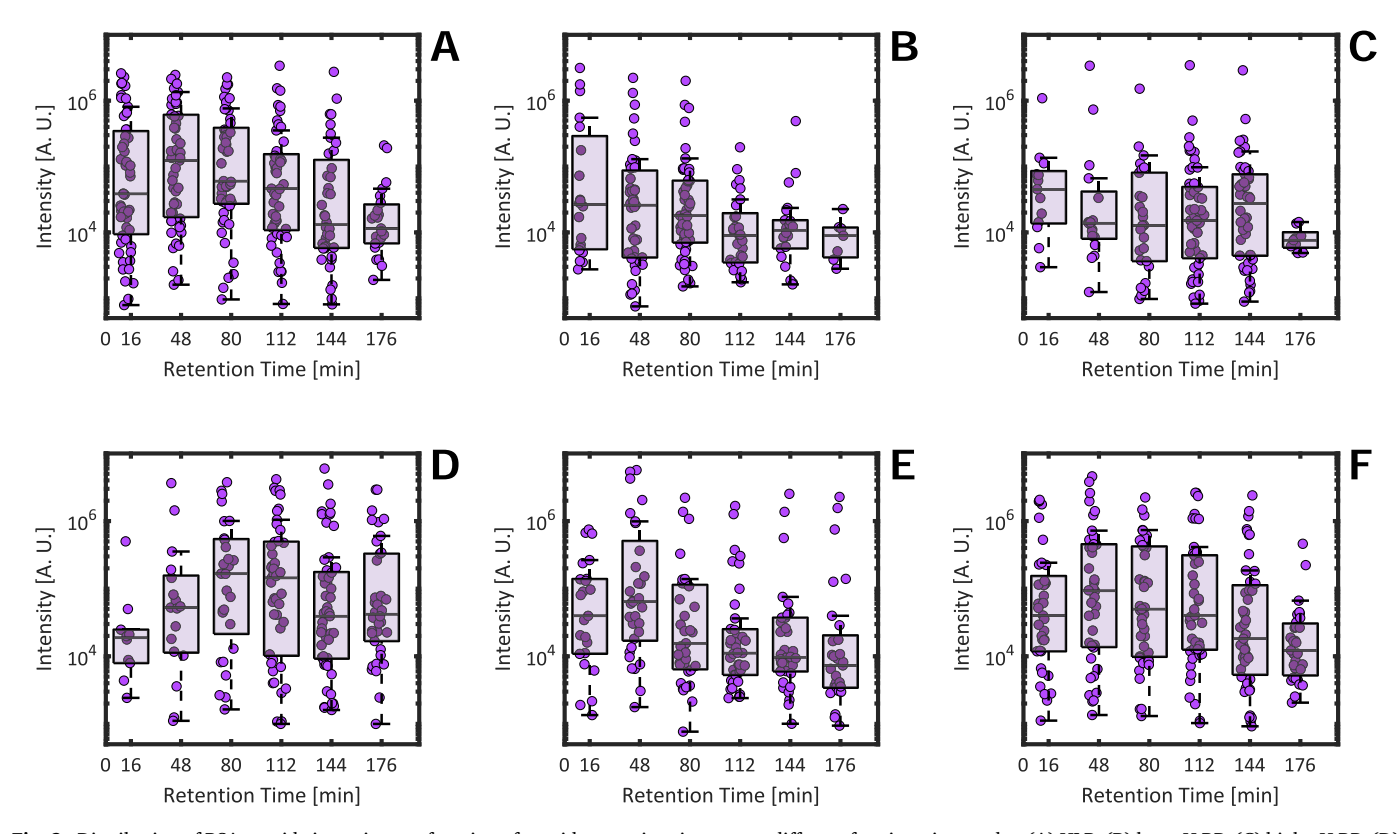


Fig. 1. Base peak intensity (BPI) chromatograms of six BSA tryptic peptide fractions obtained by offline MAX fractionation and analyzed by nanoUPLC-ESI-QTOF instrument. Each chromatogram represents one fraction: (A) Fraction 1, (B) Fraction 2, (C) Fraction 3, (D) Fraction 4, (E) Fraction 5, and (F) Fraction 6.



**Fig. 2.** Distribution of BSA peptide intensity as a function of peptide retention time across different fractionation modes: (A) HLB, (B) low pH RP, (C) high pH RP, (D) SCX, (E) QMA and (F) MAX. Retention time (in minutes) is shown on the x-axis, and peptide intensity on the y-axis. A.U. – arbitrary units. Each circle represents an individual peptide. In the boxplot, the central line marks the median, the box encloses the inter-quartile range (25th -75th percentiles), and the whiskers extend to the most extreme values that lie within 1.5 × IQR of the quartiles (values beyond this range are treated as outliers).

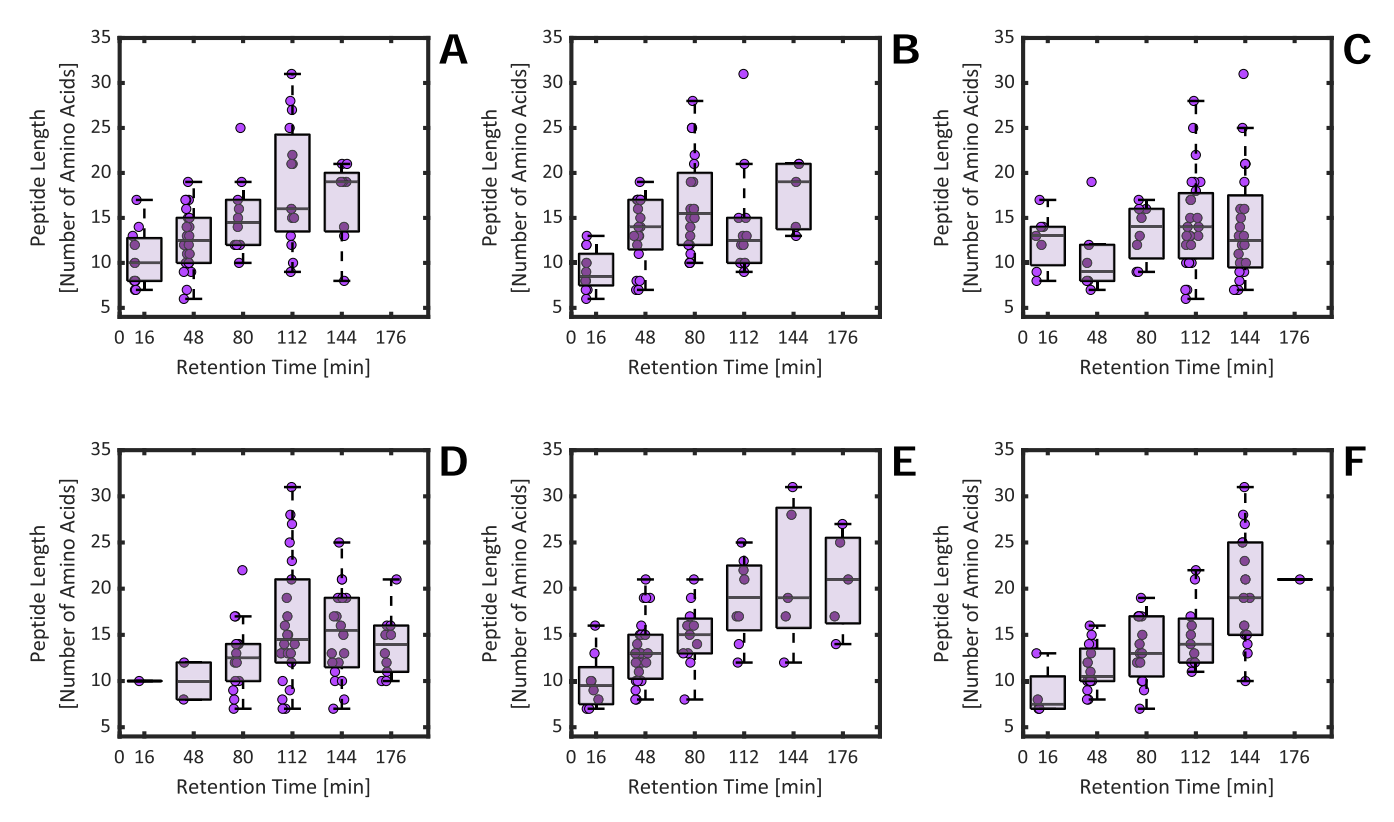


Fig. 3. Distribution of BSA peptide length as a function of peptide retention time across different fractionation modes: (A) HLB, (B) low pH RP, (C) high pH RP, (D) SCX, (E) QMA and (F) MAX. Peptides detected in multiple fractions were assigned to the most probable elution fraction based on their intensity distribution (see Methods). Retention time (in minutes) is shown on the x-axis, and peptide length (number of amino acids) on the y-axis. Circles and boxplots are as described in Fig. 2.

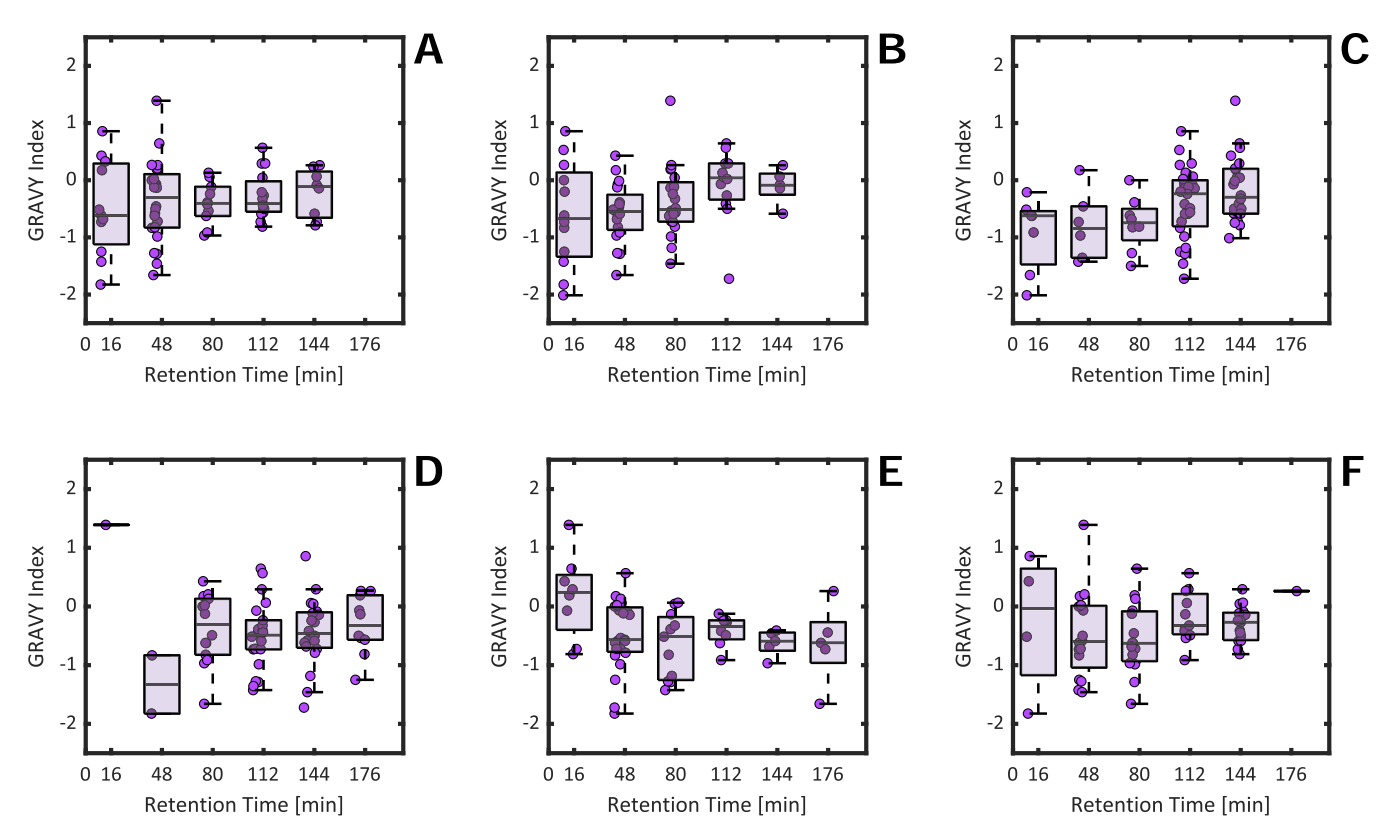


Fig. 4. Distribution of BSA peptide GRAVY index as a function of peptide retention time across different fractionation modes: (A) HLB, (B) low pH RP, (C) high pH RP, (D) SCX, (E) QMA and (F) MAX. Peptides detected in multiple fractions were assigned to the most probable elution fraction based on their intensity distribution (see Methods). Retention time (in minutes) is shown on the x-axis, and the peptide GRAVY index on the y-axis. Circles and boxplots are as described in Fig. 2.

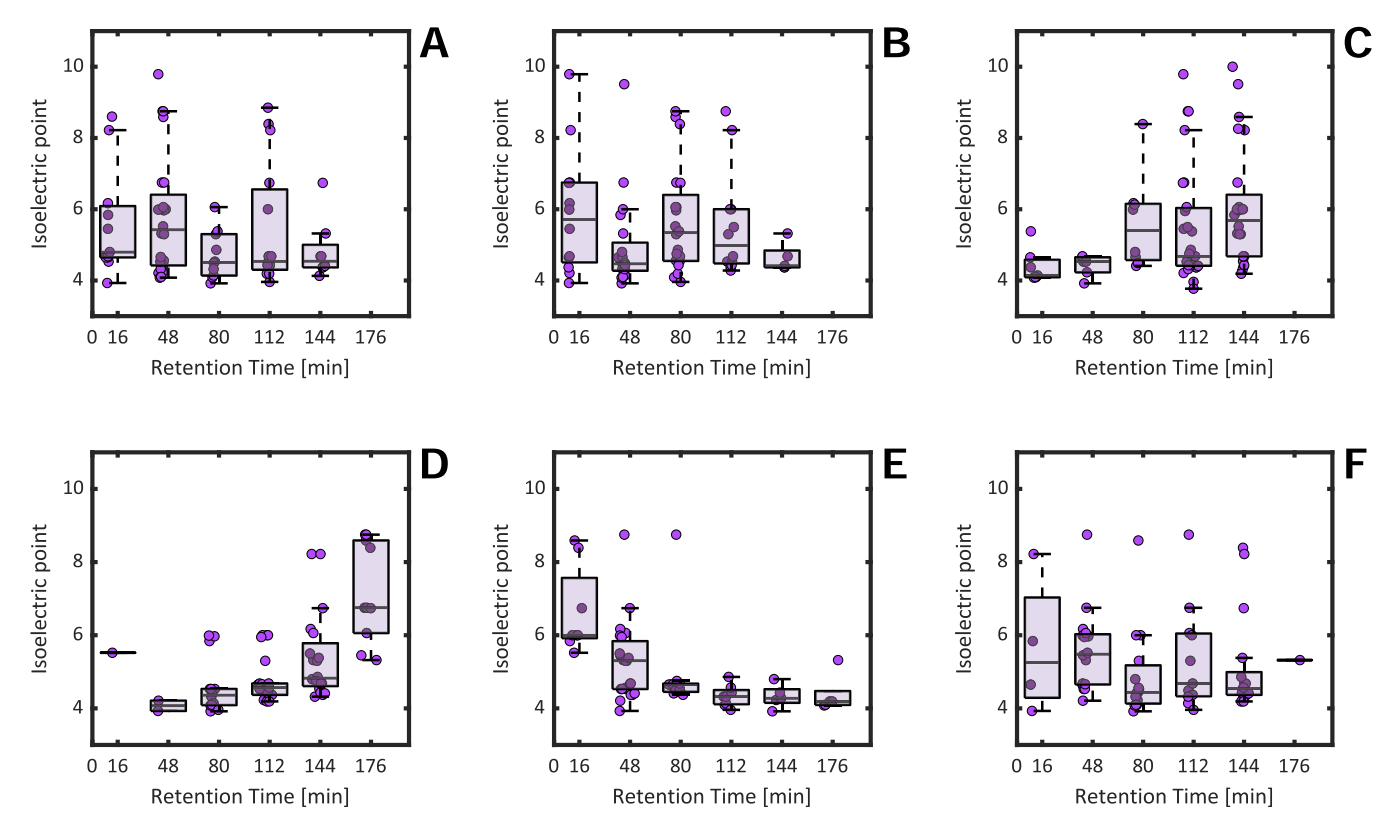


Fig. 5. Distribution of BSA peptide isoelectric point as a function of peptide retention time across different fractionation modes: (A) HLB, (B) low pH RP, (C) high pH RP, (D) SCX, (E) QMA and (F) MAX. Peptides detected in multiple fractions were assigned to the most probable elution fraction based on their intensity distribution (see Methods). Retention time (in minutes) is shown on the x-axis, and the peptide isoelectric point on the y-axis. Circles and boxplots are as described in Fig. 2.

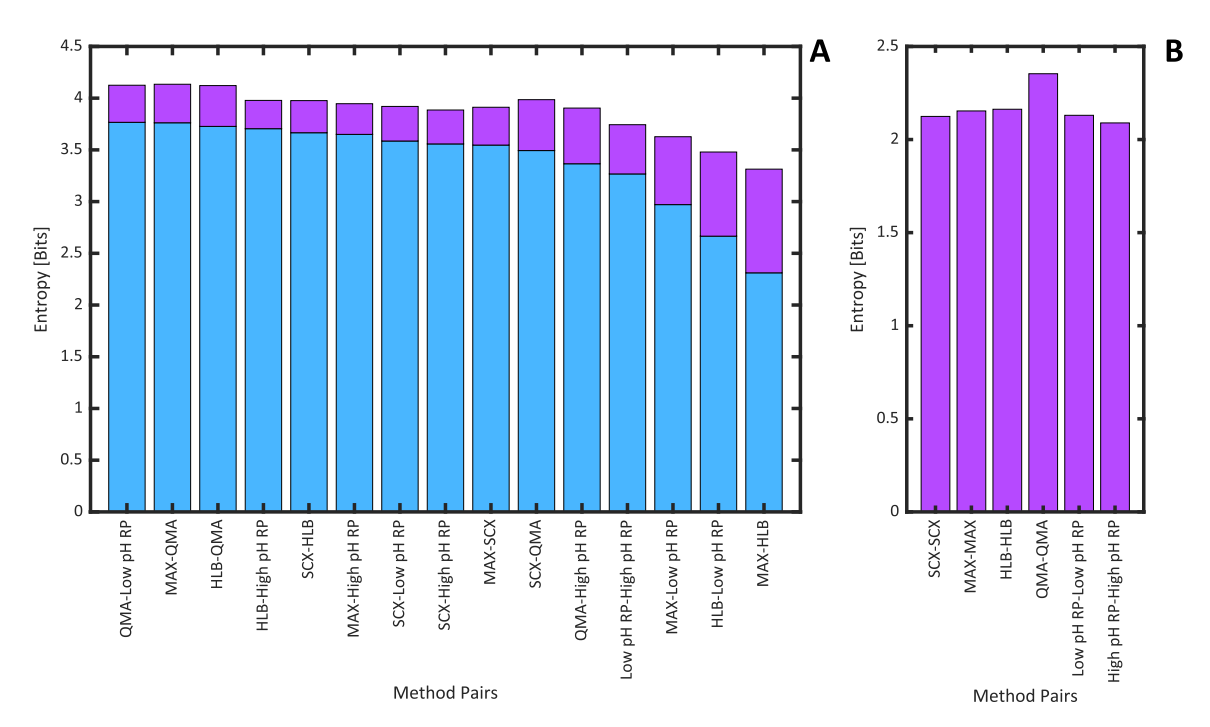


Fig. 6. Joint entropy and mutual information for combinations of peptide fractionation methods. (A) Method pairs using different column types, and (B) pairs with the same column type. The total bar height (blue + purple) indicates the joint entropy (M1, M2). The purple portion represents the mutual information (M1; M2) and the blue portion corresponds to the sum of the conditional entropies, (M1 | M2) + (M2 | M1). For the same-column comparisons in (B), the purple area corresponds to the entropy of single method, as joint entropy collapses to the marginal entropy for identical inputs. The method pairs are listed along the x-axis, and the y-axis denotes the value in bits.

(Fig. 5A). In contrast, peptide retention in both low and high pH RP was affected by peptide pI (Fig. 5B and 5C). As previously reported [13], the pH of the mobile phase has a pronounced effect on peptide retention in RPLC, with low pH and high pH RP modes exhibiting opposing trends; acidic peptides are more strongly retained at low pH (pH 2.5), while basic peptides show increased retention at high pH (pH 10).

While hydrophilic and hydrophobic interactions contribute to peptide retention in IEX [46], Fig. 5 D and 5E highlight that separation in SCX and QMA is primarily driven by peptide pI. SCX strongly retains basic peptides which elute in later fractions due to stronger electrostatic interactions with the negatively charged sorbent, whereas QMA retains acidic peptides more strongly, consistent with its positively charged sorbent, indicating complementary selectivity between the two methods.

MAX, as a mixed-mode sorbent, combines hydrophobic and ionic interactions for peptide separation [47]. As a result, peptide distributions based on both GRAVY index and pI show no consistent trends across fractions (Figs. 4F and 5F). However, it can be observed that later fractions contain more hydrophobic peptides with lower pI values, which aligns with the dual retention mechanism of the MAX sorbent.

#### 3.3. Peptide fractionation efficiency in 1D-µSPE

Peptide fractionation efficiency in 1D-µSPE was finally assessed by calculating entropy values for each fractionation method. Entropy was used as an indicator of how evenly peptides were spread across six fractions, with higher entropy reflecting more balanced peptide distribution [35,36]. At this point, the effect of peptide physicochemical properties was not considered; instead, entropy values were computed solely based on the adjusted peptide retention times, represented as mean fractions for each dimension. To allow for comparison between methods, entropy values were calculated using the same random variable definitions with six fractions. All tested methods showed comparable entropy values, indicating balanced peptide distribution across fractions (Fig. 6B). Among them, QMA fractionation exhibited the highest entropy (2.35 bits), indicating the most even peptide distribution across fractions when charge-based fractionation is employed. In contrast, high pH RP yielded the lowest entropy, implying that peptides were concentrated in fewer fractions and providing less effective separation under these conditions. The stability and function of peptides are significantly affected in alkaline environments, often leading to decreased solubility and increased aggregation which can interfere with their separation during high pH RP chromatography. Namely, not only are peptide bonds susceptible to hydrolysis under alkaline conditions, but chemical modifications - such as asparagine and glutamine deamidation can also alter the overall charge and structure of peptides, thereby affecting peptide retention behaviour [48]. Therefore, to evaluate peptide stability under different pH conditions, we compared the number of peptide chemical modifications - methionine oxidation, serine and threonine dehydration, asparagine and glutamine deamidation, and C-terminus amidation following low and high pH RP fractionation (Table 2). The analysis revealed an approximately 13 % increase in the total number of degradation modifications at pH 10

Table 2 Comparison of BSA tryptic peptide modification sites across fractions obtained by low pH and high pH RP PP- $\mu$ SPE. Results are expressed as the percentage of the total number of identified peptides. M – methionine, S – serine, T - threonine, N – asparagine, Q – glutamine.

| Modification (%) | Low pH RP | High pH RP |
|------------------|-----------|------------|
| Oxidation M      | 5.1       | 4.0        |
| Dehydration ST   | 43.6      | 44.4       |
| Deamidation N    | 28.2      | 27.3       |
| Deamidation Q    | 7.7       | 15.2       |
| Amidation C-TERM | 15.4      | 9.1        |
| Total %          | 34.7      | 47.6       |

compared to pH 2.5, with most pronounced difference noted for glutamine deamidation at high pH, and C-terminal amidation at low pH. Both acidic and basic conditions can induce chemical modifications in amide groups which can lead to peptide and protein destabilization. Specifically, acidic pH promotes hydrolysis, while alkaline pH favours intramolecular cyclization [49,50]. Although asparagine residues are typically more susceptible to deamidation under physiological conditions, our results also showed a marked increase in glutamine deamidation under high pH conditions. Recent studies suggest that alkaline environments can significantly accelerate glutamine deamidation, which has been attributed to changes in the ionization state of catalytic groups [51] as well as direct hydrolysis catalyzed by OH-/H2O [52]. In addition, interactions between peptides and the polymer-based C18 sorbent may further promote glutamine deamidation at high pH, as the porous polymer structure can enhance peptide-sorbent interactions and increase side-chain exposure to hydroxide ions. This modification can progressively impair protein structural integrity and biological activity, and increase the possibility for aggregation [53]. Notably, analysis of the peptide fractions following high pH RP fractionation led to a sharp increase in analytical column backpressure, indicating possible precipitation and accumulation of peptide aggregates. This suggests that fractionation under high pH conditions induces peptide instability or aggregation, potentially compromising downstream LC-MS performance and raising concerns about the practicality of high pH RP in multidimensional workflows.

# 3.4. Evaluation of separation orthogonality in 2D-µSPE

Several quantitative orthogonality metrics have been employed to evaluate separation orthogonality between different stationary phases and separation mode pairs in analytical chromatography [31,32,54–57]. However, comprehensive analysis of different metric approaches showed that there is no perfect method that explains the data variance. Moreover, it was shown that some approaches favour certain 2D distributions [32]. Most of the methods have been developed for online 2D chromatographic systems, utilizing both discretized and non-discretized metrics. In an offline setup with a finite number of fractions per dimension, as applied in this research, discretized approach deemed particularly suitable. We computed Shannon entropies H(A),H(B),H(A, B)H(A), H(B), H(A,B)H(A),H(B),H(A,B) and mutual information I(A;B)I (A;B)I(A;B) from the  $6 \times 6$  peptide contingency tables for each method pair, interpreting orthogonality as maximal joint entropy and minimal MI (independence), a formulation recommended for discretized separations and used previously in 2D-LC orthogonality studies [35,58].

As defined in the Methods section, entropy can be interpreted as the number of bits of information required to identify which fraction a peptide occupies. In practical terms, each bit corresponds to the answer to a "yes/no" question. Consequently, higher entropy implies greater uncertainty about a peptide's fraction assignment, since more questions must be answered to pinpoint it. Conversely, mutual information measures how much the knowledge of one method's fraction assignment reduces the uncertainty in another method's fraction assignment. Hence, when assessing orthogonality between two methods, maximal entropy is desirable (i.e., high uncertainty in any one method alone) but minimal mutual information (i.e., little overlap or dependence between the methods).

Another useful perspective—illustrated in the graphical abstract—is that the joint entropy  $H(M_1,M_2)$  can be decomposed into the sum of two conditional entropies  $H(M_1|M_2)$ , and  $H(M_2|M_1)$ , plus the mutual information  $I(M_1,M_2)$ . One can thus design a simple measure of orthogonality by taking the difference between entropy and mutual information: maximizing this difference corresponds to maximizing the sum of the conditional entropies.

The results of this approach are shown in Fig. 6A. Notably, the entropy values for the method pairs are nearly the same, with a standard deviation of 0.21 bits. Similarly, the mutual information has standard

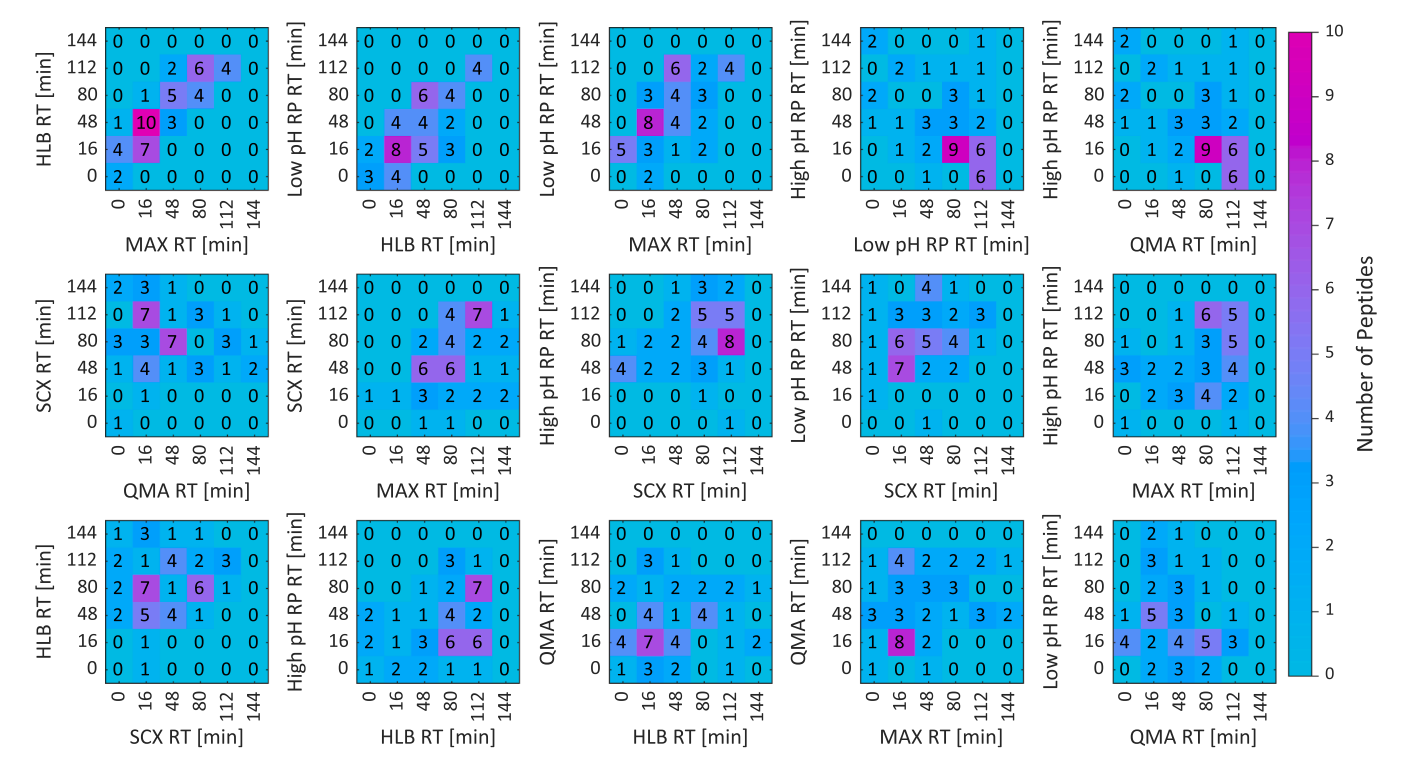


Fig. 7. Orthogonality plots for 2D-μSPME peptide fractionation using heat maps representing the number of identified peptides per fraction. Each heat map represents a pairwise column combination, with corresponding fraction retention times plotted along the axes. Color intensity reflects the number of peptides identified in each fraction intersection, with a gradient scale indicating peptide count.

deviation of 0.20 bits, but the relative difference between some pairs is 2- or 3-fold, which allows for scoring of the orthogonality.

Specifically, the top nine fractionation pairs exhibited closely matched high entropy and mutual information values, making further discrimination between them challenging (Fig. 6A). These combinations showed dispersed peptide distributions across the 2D separation space (Fig. 7), highlighting their potential utility in multidimensional peptide fractionation protocols. Most of these pairings combine ion exchange with hydrophobicity-based separation modes, such as QMA-low pH RP, HLB-QMA, HLB-high pH RP, SCX-HLB, and SCX-low pH RP. These results highlight the key advantage of offline µSPE multidimensional workflows, a simple combination of truly orthogonal fractionation protocols which utilize conditions incompatible with following online RPLC in 2D protocols or direct coupling to LC-MS – such as buffers with high salt content or extreme pH that drive peptide elution from ionexchange columns. MAX, a mixed-mode sorbent, demonstrated the best performance when paired with QMA, an ion-exchange sorbent, suggesting predominantly hydrophobic interaction-driven peptide separation in the first dimension. Moreover, high orthogonality was also observed in MAX-high pH RP and MAX-SCX combinations, both providing comparable fractionation performance. Among these, the SCX-low pH RP combination is well-established approach in 2D peptide separation for shotgun proteomics, known as Multi-Dimensional Protein Identification Technology (MudPIT) [59]. Other combinations, although not vet widely adopted in multidimensional workflows, show considerable promise for improving proteome coverage. For example, HLB sorbent, which previously showed excellent results for phosphopeptides purification [30], appears efficient in peptide separation when paired with strong ion exchange columns. Moreover, QMA-based separations particularly stand out because of their highest one-dimensional entropy values which become even more apparent in 2D combinations with RP-based modes, indicating robust and even peptide partitioning.

Our scoring system suggests that the combination of SCX-QMA and QMA-high pH RP should be considered less orthogonal, as evidenced by a relatively large fraction of total entropy that is contributed by mutual

information (Fig. 6A). This is also evident in the corresponding heat maps which display uneven clustering patterns indicating a suboptimal occupation of the 2D separation space (Fig. 7). Although QMA, as a strong anion exchanger, might be expected to offer complementary selectivity to SCX, the observed peptide overlap suggests co-elution of structurally related peptide subsets. In the Yin-Yang multidimensional LC approach, developed for separation of peptides with wide-spread pI values, SCX and SAX prefractionation strategies are combined prior the RPLC-MS analysis [60]. While this approach may hold promise in phosphoproteomics, our results indicate substantial redundancy in combining fractionation modes that do not utilize orthogonal physicochemical properties, such as these purely charge-based separations, for whole-proteome profiling. Finally, the method pairs low pH RP-high pH RP, MAX-low pH RP, HLB-low pH RP, and MAX-HLB appear more dependent than the others, with lowest entropy and highest mutual information. The corresponding heat maps reveal pronounced clustering of peptides along the main diagonal, indicating a high degree of redundancy between the combined fractionation modes, which was expected given their non-orthogonal separation mechanisms (Fig. 7). Despite the widespread use of high pH RP-low pH RP combination in shotgun proteomics, and multiple papers highlighting its separation efficiency in 2D-LC [10,13,42,61], our evaluation revealed this pairing to be the least orthogonal among all tested combinations. Significant variation in the buffer pH undoubtedly affected charged peptide retention selectivity during RPLC, as shown by the peptide distribution dependent on pI. However, hydrophobic interactions still represent a considerable component lowering the overall orthogonality of this combination. Moreover, the increased number of peptide modifications and reduced peptide stability under alkaline conditions observed in this study further highlight the practical drawbacks of implementing high pH RP in multidimensional peptide fractionation protocols.

# 3.5. Implementation of automated $\mu SPE$ for optimized peptide fractionation

Compared to conventional SPE cartridges that require manual handling and relatively large sample consumption and dissipation,  $\mu SPE$ allows for high peptide recovery ( $\approx 95$  %) of minimal sample load (as little as 10 µg of protein digest, as shown in this research). Moreover, improved sensitivity and seamless integration into automated proteomics workflows are additional benefits, which is especially important for clinical samples and pharmaceuticals where maintaining the analyte concentration is crucial. To demonstrate the practical utility of the automated PP-µSPE fractionation workflow, we analyzed Fab fragment of Cetuximab, a mAb used for the treatment of metastatic colorectal cancer, head and neck cancer and non-small cell lung cancer [62]. Confirming the protein sequence of mAbs used as therapeutics is the first step in their characterization needed for patent protection, regulatory approval and quality control [63]. Compared to typical proteins, mAbs are structurally more complex, require more elaborate sample preparation, often combined with multiple proteomic strategies (bottom-up, middle-down and top-down) to obtain the full sequence [64].

In our study, Cetuximab tryptic peptides were first analyzed after standard C18 clean-up, which yielded complete sequence coverage of the Fab light chain, but only 95.9 % coverage of the Fab heavy chain, with the C-terminal part (VDKREPKS) undetected (Table S2, Table S3). To address this gap, Cetuximab digest was subjected to QMA fractionation using the proposed PP-µSPE protocol (Table 1), which demonstrated the best results in 1D. QMA fractionation enabled identification of the previously missing heavy chain peptide in the first fraction (Table S4), resulting in 100 % sequence coverage of both light and heavy chains of the Cetuximab Fab fragment. Moreover, VDKREPKS peptide elution in the QMA fraction 1, considering its length (9 amino acids) and pI ( $\sim$ 8), is in line with the trends observed for BSA peptide fractionation which showed fraction 1 populated with shorter peptides with higher pI values (Figs. 3E, 5E). This consistency across proteins underscores the role of peptide pI value and length as determining factors in peptide QMA fractionation and offers a robust framework for interpreting peptide distribution across different proteins.

# 3.6. Advantages and considerations of automated PP-µSPE

In contrast to other commonly used small-scale SPE formats such as ZipTips [65,66], StageTips [67] or negative pressure SPE systems, PP-µSPE systems are easy to automate and extremely reliable in terms of reproducibility. The automation offers precise control over flow and volume, minimizing sample loss and ensuring high fraction-to-fraction reproducibility which enables standardization across different samples in quantitative pipelines. This was confirmed by plotting the retention times of two replicate HLB experiments (Fig. S1). Additionally, µSPE can be integrated into multi-step workflows, including on-cartridge digestion and chemical labelling (e.g. Tandem Mass Tag, TMT or Isobaric Tags for Relative and Absolute Quantitation, iTRAQ) which can reduce overall sample processing time and improve downstream MS performance. Beyond Agilent's AssayMAP Bravo, used in this research, there are other liquid handling platforms available on the market (e.g. Thermo Fisher's Versette, Opentrons OT-2, Tecan's Freedom EVO/Fluent, Beckman Coulter's Biomek, Perkin Elmer's Janus or Hamilton's Microlab STAR) which support µSPE protocols and enable for an easy transfer of multidimensional peptide fractionation protocols across different facilities.

A frequently noted limitation for offline peptide fractionation is the increase in overall analysis time, as each obtained fraction requires a separate LC-MS run. For 36 fractions, like in our envisioned protocol, this significantly extends the instrument use as well as subsequent data analysis. However, automated offline fractionation allows for selective LC-MS strategies, like fraction concatenation which can reduce the number of injections by combining non-adjacent fractions with

complementary peptide elution profiles [40]. Additionally, sample fractionation enables targeted analysis of only relevant fractions when elution profile of a peptide of interest is known. This is particularly relevant in workflows using selected reaction monitoring (SRM) and multiple reaction monitoring (MRM), where protein identification relies on predefined proteotypic peptides [68,69]. In such cases, reproducible and optimized peptide fractionation, coupled with accurate peptide retention prediction, can substantially enhance both the sensitivity and accuracy of protein identification and quantification.

# 4. Conclusions

Orthogonality of separation in 2D-µSPE underscores the advantages of automated PP-µSPE workflows for flexible, scalable, and reproducible peptide fractionation enabling reduction of proteome complexity and implementation in targeted protein analysis workflows, with its key advantage of combining truly orthogonal separation chemistries within multidimensional chromatography protocols. Systematic evaluation of six fractionation modes highlighted the role of peptide physicochemical properties (pI, length, and hydrophobicity) in peptide distribution profiles. Entropy and mutual information analyses provided quantitative insights into the complementarity of column pairs. Among all tested methods, QMA exhibited the highest entropy, indicating superior separation efficiency in the first dimension. Combinations of QMA with MAX, low pH RP, or HLB, achieved the highest cumulative entropy and the lowest mutual information, indicating enhanced orthogonality and minimal overlap in peptide profiles across dimensions. These results emphasize the importance of combining different and complementary separation chemistries to improve peptide resolution and subsequent protein coverage in multidimensional workflows or to accurately extract peptides in targeted proteomics analysis.

The practical utility of PP-uSPE was demonstrated using Fab fragment of Cetuximab, where QMA fractionation enabled identification of a previously undetected heavy chain peptide, achieving complete sequence coverage and highlighting the workflow's applicability to complex therapeutic proteins. Furthermore, the observed systematic correlations between peptide retention and physicochemical properties support predictive modeling to streamline method development and optimize fraction selection in multidimensional 2D-µSPE workflows.

# **Funding**

This work was supported by European Union NextGenerationEU, National Recovery and Resilience Plan's project MetaPatvor (Grant number NPOO.C3.2.R3-I1.04.0122).

# CRediT authorship contribution statement

Renata Biba: Writing – original draft, Visualization, Methodology, Investigation, Formal analysis, Data curation. Karla Košpić: Writing – review & editing, Methodology, Investigation, Data curation. Blaž Ivšić: Writing – original draft, Visualization, Validation, Methodology, Formal analysis. Lucija Vujević: Writing – review & editing. Amela Hozić: Writing – review & editing, Project administration. Marijana Erk: Writing – review & editing, Project administration. Irena Đapić: Writing – review & editing, Mario Cindrić: Writing – review & editing, Supervision, Funding acquisition, Conceptualization.

# **Declaration of competing interest**

The authors have no relevant financial or non-financial interests to disclose.

# Supplementary materials

Supplementary material associated with this article can be found, in

the online version, at doi:10.1016/j.jcoa.2025.100262.

### Data availability

Data will be made available on request.

#### References

- M. Pirmoradian, H. Budamgunta, K. Chingin, B. Zhang, J. Astorga-Wells, R. A. Zubarev, Rapid and deep human proteome analysis by single-dimension shotgun proteomics, Mol. and Cell. Proteomics 12 (2013) 3330–3338, https://doi.org/ 10.1074/mcp.0113.028787.
- [2] Y. Zhang, B.R. Fonslow, B. Shan, M.C. Baek, J.R. Yates, Protein analysis by shotgun/bottom-up proteomics, Chem. Rev. 113 (2013) 2343–2394, https://doi. org/10.1021/cr3003533.
- [3] E.M. Solovyeva, A.A. Lobas, A.T. Kopylov, I.Y. Ilina, L.I. Levitsky, S. A. Moshkovskii, M.V. Gorshkov, FractionOptimizer: a method for optimal peptide fractionation in bottom-up proteomics, Anal. Bioanal. Chem. 410 (2018) 3827–3833, https://doi.org/10.1007/s00216-018-1054-2.
- [4] L. Deng, D.C.L. Handler, D.H. Multari, P.A. Haynes, Comparison of protein and peptide fractionation approaches in protein identification and quantification from *Saccharomyces cerevisiae*, J. Chromatogr. B Analyt. Technol. Biomed. Life Sci. (2021) 1162, https://doi.org/10.1016/j.jchromb.2020.122453.
- [5] Y. Fukao, M. Yoshida, R. Kurata, M. Kobayashi, M. Nakanishi, M. Fujiwara, K. Nakajima, A. Ferjani, Peptide separation methodologies for in-depth proteomics in Arabidopsis, Plant Cell Physiol. 54 (2013) 808–815, https://doi.org/10.1093/ pcp/pct033.
- [6] S. Bandhakavi, T.W. Markowski, H. Xie, T.J. Griffin, Three-dimensional peptide fractionation for highly sensitive nanoscale LC-based shotgun proteomic analysis of complex protein mixtures. Methods in Molecular Biology, Humana Press Inc., 2011, pp. 47–56, https://doi.org/10.1007/978-1-61779-319-6\_4.
- [7] B. Manadas, V.M. Mendes, J. English, M.J. Dunn, Peptide fractionation in proteomics approaches, Expert Rev. Proteomics 7 (2010) 655–663, https://doi. org/10.1586/epr.10.46.
- [8] L.M. Patil, D.H. Parkinson, N.R. Zuniga, H.J.L. Lin, B.C. Naylor, J.C. Price, Combining offline high performance liquid chromatography fractionation of peptides and intact proteins to enhance proteome coverage in bottom-up proteomics, J. Chromatogr. A (2023) 1701, https://doi.org/10.1016/j. chroma.2023.464044.
- [9] S. Di Palma, M.L. Hennrich, A.J.R. Heck, S. Mohammed, Recent advances in peptide separation by multidimensional liquid chromatography for proteome analysis, J. Proteomics 75 (2012) 3791–3813, https://doi.org/10.1016/j. jprot.2012.04.033.
- [10] D. Yeung, B. Mizero, D. Gussakovsky, N. Klaassen, Y. Lao, V. Spicer, O.V. Krokhin, Separation orthogonality in liquid chromatography-mass spectrometry for proteomic applications: Comparison of 16 different two-dimensional combinations, Anal. Chem. 92 (2020) 3904–3912, https://doi.org/10.1021/acs. analchem.9b05407.
- [11] M.Z. Zhu, N. Li, Y.T. Wang, N. Liu, M.Q. Guo, B.Q. Sun, H. Zhou, L. Liu, J.L. Wu, Acid/salt/pH gradient improved resolution and sensitivity in proteomics study using 2D SCX-RP LC-MS, J. Proteome Res. 16 (2017) 3470–3475, https://doi.org/ 10.1021/acs.jproteome.7b00443.
- [12] D. Tao, X. Qiao, L. Sun, C. Hou, L. Gao, L. Zhang, Y. Shan, Z. Liang, Y. Zhang, Development of a highly efficient 2-D system with a serially coupled long column and its application in identification of rat brain integral membrane proteins with ionic liquids-assisted solubilization and digestion, J. Proteome Res. 10 (2011) 732–738. https://doi.org/10.1021/pr100893i.
- [13] M. Gilar, P. Olivova, A.E. Daly, J.C. Gebler, Two-dimensional separation of peptides using RP-RP-HPLC system with different pH in first and second separation dimensions, J. Sep. Sci. 28 (2005) 1694–1703, https://doi.org/10.1002/ jssc.200500116.
- [14] G.J. Opiteck, J.W. Jorgenson, Two-dimensional SEC/RPLC coupled to mass spectrometry for the analysis of peptides, Anal. Chem. 69 (1997) 2283–2291, https://doi.org/10.1021/ac961156d.
- [15] H.J. Lee, K. Na, M.S. Kwon, T. Park, K.S. Kim, H. Kim, Y.K. Paik, A new versatile peptide-based size exclusion chromatography platform for global profiling and quantitation of candidate biomarkers in hepatocellular carcinoma specimens, Proteomics 11 (2011) 1976–1984, https://doi.org/10.1002/pmic.201100002.
   [16] S. Di Palma, P.J. Boersema, A.J.R. Heck, S. Mohammed, Zwitterionic hydrophilic
- [16] S. Di Palma, P.J. Boersema, A.J.R. Heck, S. Mohammed, Zwitterionic hydrophilic interaction liquid chromatography (ZIC-HILIC and ZIC-cHILIC) provide high resolution separation and increase sensitivity in proteome analysis, Anal. Chem. 83 (2011) 3440–3447, https://doi.org/10.1021/ac103312e.
- [17] J.L. Cao, S.S. Wang, H. Hu, C.W. He, J.B. Wan, H.X. Su, Y.T. Wang, P. Li, Online comprehensive two-dimensional hydrophilic interaction chromatography × reversed-phase liquid chromatography coupled with hybrid linear ion trap Orbitrap mass spectrometry for the analysis of phenolic acids in *Salvia miltiorrhiza*, J. Chromatogr. A 1536 (2018) 216–227, https://doi.org/10.1016/j.chroma.2017.09.041.
- [18] Q. Wu, H. Yuan, L. Zhang, Y. Zhang, Recent advances on multidimensional liquid chromatography-mass spectrometry for proteomics: From qualitative to quantitative analysis - A review, Anal. Chim. Acta 731 (2012) 1–10, https://doi. org/10.1016/j.aca.2012.04.010.

- [19] V.A. Duong, J.M. Park, H. Lee, Review of three-dimensional liquid chromatography platforms for bottom-up proteomics, Int. J. Mol. Sci. 21 (2020), https://doi.org/ 10.3390/ijms21041524.
- [20] Y. Wang, F. Yang, M.A. Gritsenko, Y. Wang, T. Clauss, T. Liu, Y. Shen, M. E. Monroe, D. Lopez-Ferrer, T. Reno, R.J. Moore, R.L. Klemke, D.G. Camp, R. D. Smith, Reversed-phase chromatography with multiple fraction concatenation strategy for proteome profiling of human MCF10A cells, Proteomics 11 (2011) 2019–2026, https://doi.org/10.1002/pmic.201000722.
- [21] J. Huang, F. Wang, M. Ye, H. Zou, Enrichment and separation techniques for large-scale proteomics analysis of the protein post-translational modifications, J. Chromatogr. A 1372 (2014) 1–17, https://doi.org/10.1016/j. chroma.2014.10.107
- [22] H. Keshishian, M.W. Burgess, M.A. Gillette, P. Mertins, K.R. Clauser, D.R. Mani, E. W. Kuhn, L.A. Farrell, R.E. Gerszten, S.A. Carr, Multiplexed, quantitative workflow for sensitive biomarker discovery in plasma yields novel candidates for early myocardial injury, Mol. Cell. Proteomics 14 (2015) 2375–2393, https://doi.org/10.1074/mcp.M114.046813.
- [23] M. Smoluch, P. Mielczarek, A. Drabik, J. Silberring, Online and offline sample fractionation. Proteomic profiling and analytical chemistry: The Crossroads: Second Edition, Elsevier Inc., 2016, pp. 63–99, https://doi.org/10.1016/B978-0-444\_6388\_1,0005\_7
- [24] T. Herraiz, V. Casal, Evaluation of solid-phase extraction procedures in peptide analysis, J. Chromatogr. A 708 (1995) 209–221, https://doi.org/10.1016/0021-0673(05)00398 4
- [25] E.L. De Graaf, D. Pellegrini, L.A. McDonnell, Set of novel automated quantitative microproteomics protocols for small sample amounts and its application to kidney tissue substructures, J. Proteome Res. 15 (2016) 4722–4730, https://doi.org/ 10.1021/acs.jproteome.6b00889.
- [26] M. Kuras, L.H. Betancourt, M. Rezeli, J. Rodriguez, M. Szasz, Q. Zhou, T. Miliotis, R. Andersson, G. Marko-Varga, Assessing automated sample preparation technologies for high-throughput proteomics of frozen well characterized tissues from Swedish biobanks, J. Proteome Res. 18 (2019) 548–556, https://doi.org/ 10.1021/acs.jproteome.8b00792.
- [27] J.R. Murillo, M. Kuras, M. Rezeli, T. Milliotis, L. Betancourt, G. Marko-Varga, Automated phosphopeptide enrichment from minute quantities of frozen malignant melanoma tissue, PLoS One 13 (2018), https://doi.org/10.1371/ journal.pone.0208562.
- [28] A. Takemori, Y. Kawashima, N. Takemori, Bottom-up/cross-linking mass spectrometry, Chem. Commun. 58 (2022) 775–778, https://doi.org/10.1039/ d1cc05529a.
- [29] Y.P. Huang, R.C. Robinson, F.F.G. Dias, J.M.L.N. de Moura Bell, D. Barile, Solid-phase extraction approaches for improving oligosaccharide and small peptide identification with liquid chromatography-high-resolution mass spectrometry: A case study on proteolyzed almond extract, Foods 11 (2022), https://doi.org/10.3390/foods11030340.
- [30] F. Bugyi, G. Tóth, K.B. Kovács, L. Drahos, L. Turiák, Comparison of solid-phase extraction methods for efficient purification of phosphopeptides with low sample amounts, J. Chromatogr. A (2022) 1685, https://doi.org/10.1016/j. chroma.2022.463597.
- [31] M. Gilar, P. Olivova, A.E. Daly, J.C. Gebler, Orthogonality of separation in twodimensional liquid chromatography, Anal. Chem. 77 (2005) 6426–6434, https:// doi.org/10.1021/ac050923i.
- [32] M.R. Schure, J.M. Davis, Orthogonal separations: Comparison of orthogonality metrics by statistical analysis, J. Chromatogr. A 1414 (2015) 60–76, https://doi. org/10.1016/j.chroma.2015.08.029.
- [33] S. Chapel, M. Pardon, D. Cabooter, Systematic approach to online comprehensive 2D-LC method development for organic micropollutant profiling in wastewater, J. Chromatogr. A 1749 (2025) 465861, https://doi.org/10.1016/j. chroma.2025.465861.
- [34] P.J. Slonecker, X. Li, T.H. Ridgway, J.G. Dorsey, Informational orthogonality of two-dimensional chromatographic separations, Anal. Chem. 68 (1996) 682–689, https://doi.org/10.1021/ac950852v.
- [35] M.R. Pourhaghighi, M. Karzand, H.H. Girault, Orthogonality of two-dimensional separations based on conditional entropy, Anal. Chem. 83 (2011) 7676–7681, https://doi.org/10.1021/ac2017772.
- [36] T.M. Cover, J.A. Thomas, Elements of Information Theory, John Wiley & Sons, Inc., Hoboken, NJ, 2005, https://doi.org/10.1002/047174882X.
- [37] J.C. Giddings, Sample dimensionality: a predictor of order-disorder in component peak distribution in multidimensional separation, J. Chromatogr. A 703 (1995) 3–15, https://doi.org/10.1016/0021-9673(95)00249-m.
- [38] D.R. Stoll, P.W. Carr, Two-dimensional liquid chromatography: a state of the art tutorial, Anal. Chem. 89 (2017) 519–531, https://doi.org/10.1021/acs. analchem.6b03506.
- [39] B.W.J. Pirok, A.F.G. Gargano, P.J. Schoenmakers, Optimizing separations in online comprehensive two-dimensional liquid chromatography, J. Sep. Sci. 41 (2018) 68–98, https://doi.org/10.1002/jssc.201700863.
- [40] M. Zurawska, M. Basik, A. Aguilar-Mahecha, M. Dadlez, D. Domanski, A microflow, high-pH, reversed-phase peptide fractionation and collection system for targeted and in-depth proteomics of low-abundance proteins in limiting samples, MethodsX 11 (2023), https://doi.org/10.1016/j.mex.2023.102306.
- [41] N.A. Kulak, P.E. Geyer, M. Mann, Loss-less Nano-fractionator for High Sensitivity, High Coverage Proteomics, Mol. Cell. Proteomics 16 (2017) 694–705, https://doi. org/10.1074/mcp.0116.065136.
- [42] F. Yang, Y. Shen, D.G. Camp, R.D. Smith, High-pH reversed-phase chromatography with fraction concatenation for 2D proteomic analysis, Expert Rev. Proteomics 9 (2012) 129–134, https://doi.org/10.1586/epr.12.15.

- [43] O. Al Musaimi, O.M.M. Valenzo, D.R. Williams, Prediction of peptides retention behavior in reversed-phase liquid chromatography based on their hydrophobicity, J. Sep. Sci. 46 (2023), https://doi.org/10.1002/jssc.202200743.
- [44] L. Moruz, L. Käll, Peptide retention time prediction, Mass Spectrom. Rev. 36 (2017) 615–623, https://doi.org/10.1002/mas.21488.
- [45] J. Lenčo, S. Jadeja, D.K. Naplekov, O.V. Krokhin, M.A. Khalikova, P. Chocholouš, J. Urban, K. Broeckhoven, L. Nováková, F. Švec, Reversed-phase liquid chromatography of peptides for bottom-up proteomics: A tutorial, J. Proteome Res. 21 (2022) 2846–2892, https://doi.org/10.1021/acs.jproteome.2c00407.
- [46] L.H. Betancourt, P.J. De Bock, A. Staes, E. Timmerman, Y. Perez-Riverol, A. Sanchez, V. Besada, L.J. Gonzalez, J. Vandekerckhove, K. Gevaert, SCX charge state selective separation of tryptic peptides combined with 2D-RP-HPLC allows for detailed proteome mapping, J. Proteomics 91 (2013) 164–171, https://doi.org/ 10.1016/j.jprot.2013.06.033.
- [47] K. Zhang, X. Liu, Mixed-mode chromatography in pharmaceutical and biopharmaceutical applications, J. Pharm. Biomed. Anal. 128 (2016) 73–88, https://doi.org/10.1016/j.jpba.2016.05.007.
- [48] M. Mirzaei, A. Shavandi, S. Mirdamadi, N. Soleymanzadeh, P. Motahari, N. Mirdamadi, M. Moser, G. Subra, H. Alimoradi, S. Goriely, Bioactive peptides from yeast: A comparative review on production methods, bioactivity, structurefunction relationship, and stability, Trends Food Sci. Technol. 118 (2021) 297–315, https://doi.org/10.1016/j.tifs.2021.10.008.
- [49] M.C. Manning, D.K. Chou, B.M. Murphy, R.W. Payne, D.S. Katayama, Stability of protein pharmaceuticals: An update, Pharm. Res. 27 (2010) 544–575, https://doi. org/10.1007/s11095-009-0045-6.
- [50] K.L. Zapadka, F.J. Becher, A.L. Gomes dos Santos, S.E. Jackson, Factors affecting the physical stability (aggregation) of peptide therapeutics, Interface Focus 7 (2017), https://doi.org/10.1098/rsfs.2017.0030.
- [51] K. Kato, T. Nakayoshi, E. Kurimoto, A. Oda, Computational studies on the nonenzymatic deamidation mechanisms of glutamine residues, ACS Omega 4 (2019) 3508–3513, https://doi.org/10.1021/acsomega.8b03199.
- [52] M.A. Halim, M.H. Almatarneh, R.A. Poirier, mechanistic study of the deamidation reaction of glutamine: A computational approach, J. Phys. Chem. B 118 (2014) 2316–2330, https://doi.org/10.1021/jp4107266.
- [53] M. Michiel, E. Duprat, F. Skouri-Panet, J.A. Lampi, A. Tardieu, K.J. Lampi, S. Finet, Aggregation of deamidated human βB2-crystallin and incomplete rescue by α-crystallin chaperone, Exp. Eye Res. 90 (2010) 688–698, https://doi.org/ 10.1016/j.exer.2010.02.007.
- [54] E. Van Gyseghem, B. Dejaegher, R. Put, P. Forlay-Frick, A. Elkihel, M. Daszykowski, K. Héberger, D.L. Massart, Y. Vander Heyden, Evaluation of chemometric techniques to select orthogonal chromatographic systems, J. Pharm. Biomed. Anal. 41 (2006) 141–151. https://doi.org/10.1016/j.jpba.2005.11.007.
- [55] Y. Liu, X. Xue, Z. Guo, Q. Xu, F. Zhang, X. Liang, Novel two-dimensional reversed-phase liquid chromatography/hydrophilic interaction chromatography, an excellent orthogonal system for practical analysis, J. Chromatogr. A 1208 (2008) 133–140. https://doi.org/10.1016/j.chroma.2008.08.079.

- [56] M. Gilar, J. Fridrich, M.R. Schure, A. Jaworski, Comparison of orthogonality estimation methods for the two-dimensional separations of peptides, Anal. Chem. 84 (2012) 8722–8732, https://doi.org/10.1021/ac3020214.
- [57] C.L. Bilodeau, N.A. Vecchiarello, S. Altern, S.M. Cramer, Quantifying orthogonality and separability: A method for optimizing resin selection and design, J. Chromatogr. A (2020) 1628, https://doi.org/10.1016/j.chroma.2020.461429.
- [58] M.R. Schure, J.M. Davis, Orthogonality measurements for multidimensional chromatography in three and higher dimensional separations, J. Chromatogr. A 1523 (2017) 148–161, https://doi.org/10.1016/j.chroma.2017.06.036.
- [59] M.P. Washburn, D. Wolters, J.R. Yates III, Large-scale analysis of the yeast proteome by multidimensional protein identification technology, Nat. Biotechnol. 19 (2001) 242–247, https://doi.org/10.1038/85686.
- [60] J. Dai, W.H. Jin, Q.H. Sheng, C.H. Shieh, J.R. Wu, R. Zeng, Protein phosphorylation and expression profiling by Yin-Yang multidimensional liquid chromatography (Yin-Yang MDLC) mass spectrometry, J. Proteome Res. 6 (2007) 250–262, https:// doi.org/10.1021/pr0604155.
- [61] Z. Wang, H. Ma, K. Smith, S. Wu, Two-dimensional separation using high-pH and low-pH reversed phase liquid chromatography for top-down proteomics, Int. J. Mass Spectrom. 427 (2018) 43–51, https://doi.org/10.1016/j.ijms.2017.09.001.
- [62] Y. Humblet, Cetuximab: an IgG1 monoclonal antibody for the treatment of epidermal growth factor receptor-expressing tumours, Expert Opin. Pharmacother. 5 (2004) 1621–1633, https://doi.org/10.1517/14656566.5.7.1621.
- [63] Y. Mao, L. Zhang, A. Kleinberg, Q. Xia, T.J. Daly, N. Li, Fast protein sequencing of monoclonal antibody by real-time digestion on emitter during nanoelectrospray, MAbs 11 (2019) 767–778, https://doi.org/10.1080/19420862.2019.1599633.
- [64] L. Fornelli, K. Srzentić, R. Huguet, C. Mullen, S. Sharma, V. Zabrouskov, R. T. Fellers, K.R. Durbin, P.D. Compton, N.L. Kelleher, Accurate sequence analysis of a monoclonal antibody by top-down and middle-down orbitrap mass spectrometry applying multiple ion activation techniques, Anal. Chem. 90 (2018) 8421–8429, https://doi.org/10.1021/acs.analchem.8b00984.
- [65] A. Tiss, C. Smith, S. Camuzeaux, M. Kabir, S. Gayther, U. Menon, M. Waterfield, J. Timms, I. Jacobs, R. Cramer, Serum peptide profiling using MALDI mass spectrometry: Avoiding the pitfalls of coated magnetic beads using well-established ZipTip technology, Proteomics 7 (2007) 77–89, https://doi.org/10.1002/ pmic 200700746
- [66] T. Baczek, Fractionation of peptides in proteomics with the use of pI-based approach and ZipTip pipette tips, J. Pharm. Biomed. Anal. 34 (2004) 851–860, https://doi.org/10.1016/j.ipba.2003.11.001.
- [67] J. Rappsilber, M. Mann, Y. Ishihama, Protocol for micro-purification, enrichment, pre-fractionation and storage of peptides for proteomics using StageTips, Nat. Protoc. 2 (2007) 1896–1906, https://doi.org/10.1038/nprot.2007.261.
- [68] B. Manadas, V.M. Mendes, J. English, M.J. Dunn, Peptide fractionation in proteomics approaches, Expert Rev. Proteomics 7 (2010) 655–663, https://doi. org/10.1586/epr.10.46.
- [69] A. Bertsch, S. Jung, A. Zerck, N. Pfeifer, S. Nahnsen, C. Henneges, A. Nordheim, O. Kohlbacher, Optimal de novo design of MRM experiments for rapid assay development in targeted proteomics, J. Proteome Res. 9 (2010) 2696–2704, https://doi.org/10.1021/pr1001803.